Probabilistic Secretion of Quanta: Spontaneous Release at Active Zones of Varicosities, Boutons, and Endplates

M. R. Bennett,* W. G. Gibson,‡ and J. Robinson‡
*The Neurobiology Laboratory, Department of Physiology, and ‡The School of Mathematics and Statistics, University of Sydney, New South Wales 2006, Australia

ABSTRACT The amplitude-frequency histogram of spontaneous miniature endplate potentials follows a Gaussian distribution at mature endplates. This distribution gives the mean and variance of the quantum of transmitter. According to the vesicle hypothesis, this quantum is due to exocytosis of the contents of a single synaptic vesicle. Multimodal amplitude-frequency histograms are observed in varying degrees at developing endplates and at peripheral and central synapses, each of which has a specific active zone structure. These multimodal histograms may be due to the near synchronous exocytosis of more than one vesicle. In the present work, a theoretical treatment is given of the rise of intraterminal calcium after the stochastic opening of a calcium channel within a particular active zone geometry. The stochastic interaction of this calcium with the vesicle-associated proteins involved in exocytosis is then used to calculate the probability of quantal secretions from one or several vesicles at each active zone type. It is shown that this procedure can account for multiquantal spontaneous release that may occur at varicosities and boutons, compared with that at the active zones of motor nerve terminals.

INTRODUCTION

Spontaneous secretion of transmitter quanta occurs at synapses which use fast-acting synaptic transmitters such as acetylcholine, glutamate, γ-aminobutyric acid (GABA), and ATP acting on ionotropic receptors. The amplitude-frequency histograms of the spontaneous potentials to which these quanta give rise when recorded with an intracellular electrode vary depending on the synapse investigated rather than on the transmitter type. For example, at the amphibian neuromuscular junction where spontaneous potentials were first described, the amplitude-frequency histogram is Gaussian (Fatt and Katz, 1952). In contrast, at preganglionic synapses on amphibian sympathetic ganglia the amplitude-frequency histogram is often not Gaussian (Blackman et al., 1963), but may be better fitted by a gamma-distribution (Robinson, 1976). Indeed, histograms of spontaneous potentials at mammalian preganglionic synapses may be better described as showing several modes that are integer multiples of the unit mode, indicating multiquantal release (Blackman and Purves, 1969; Bornstein, 1981), and it is for this reason that they are better fitted by a gamma than by a Gaussian distribution. Histograms of spontaneous potentials that may indicate multiquantal release have also been observed at inhibitory nerve terminals releasing GABA onto hippocampal granule cells (Edwards et al., 1990) as well as at mossy fiber terminals releasing glutamate onto cerebellar granule cells (Silver et al., 1992) and optic nerve terminals releasing glutamate onto lateral geniculate nucleus cells (Paulsen and Heggelund, 1994). Recently, attempts have been made to record from individual release sites of nerve terminals. Experiments in which a few boutons on hippocampal pyramidal neurons are exposed to hypertonic solutions, and recordings made in the neuron soma of accelerated spontaneous releases from the boutons, give histograms that are better described by gamma rather than by Gaussian distributions (Bekkers et al., 1990). In other experiments, spontaneous release of ATP has been recorded from single visualized varicosities of sympathetic nerve terminals with extracellular electrodes; histograms of the potentials arising from this release are often better described by gamma than by Gaussian distributions (Bennett, 1993; Lavidis and Bennett, 1992), and most likely contain multiquantal releases (Bennett, 1994).

The question arises as to whether there is a single determining factor for the shape of amplitude-frequency histograms at different synapses. In this work we explore the possibility that differences in active zone structure might be responsible for the mixture of quantal versus multiquantal spontaneous release that seems to occur at different synapses. The active zones of nerve terminals differ markedly, depending on the synapse considered (Couteaux, 1961). At synaptic varicosities formed by sympathetic nerve terminals the active zone does not have a particular arrangement of vesicles on the presynaptic membrane (Fig. 1; Bennett, 1972; Gabella, 1992); in the absence of freeze-fracture studies the distribution of 10 nm presumptive calcium channel particles is not known. At boutons formed by nerve terminals on other neurons, the active zone consists of a presynaptic vesicular grid with dense projections among which synaptic vesicles may nestle (Akert, 1973; Triller and Korn, 1982); the 10 nm particles appear scattered throughout the grid (Fig. 2). Finally, at nerve terminals on fast twitch fibers in amphibia the active zone consists of two double parallel rows of 10 nm particles, taken to be calcium channels (Pumplin et al., 1981; Robitaille et al., 1990), flanked by synaptic vesicles (Fig. 3; Dreyer et al., 1973;

Received for publication 27 January 1995 and in final form 20 April 1995.
Address reprint requests to Dr. Max Bennett, Neurobiology Laboratory, F13, University of Sydney, New South Wales 2006, Australia. Tel.: 61-2-692-2034; Fax: 61-2-351-4740; E-mail: maxb@physiol.su.oz.au.

0006-3495/95/07/42/15 $2.00

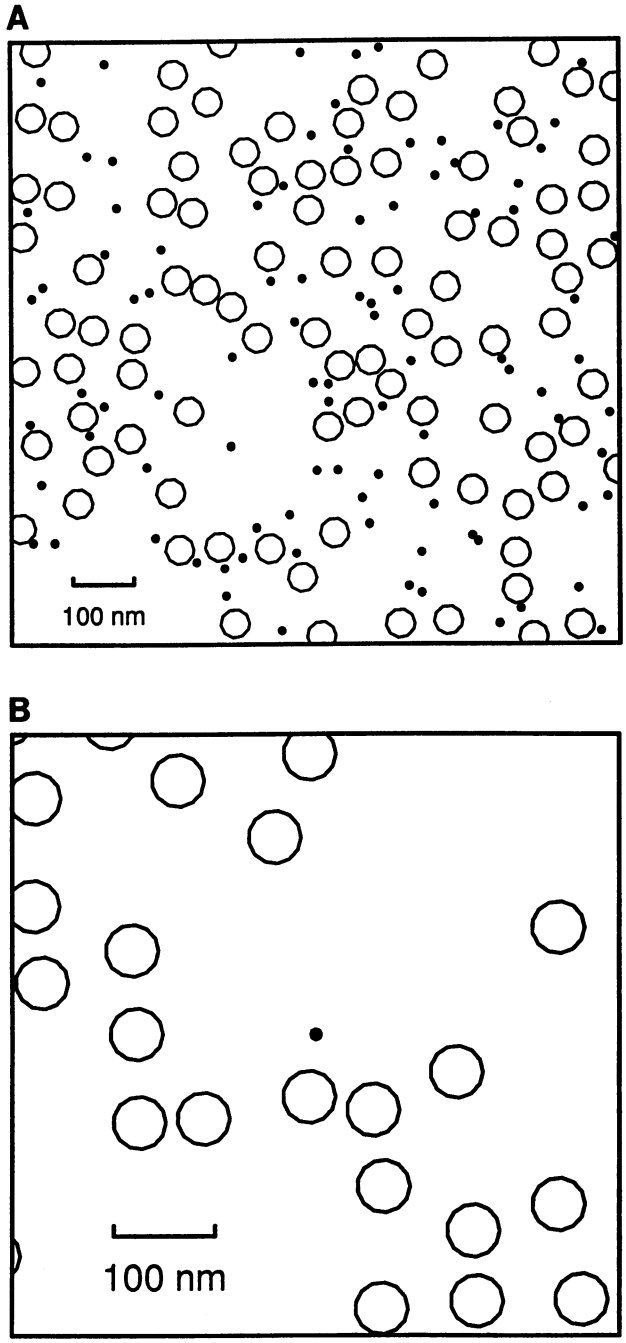

FIGURE 1 Active zone in a synaptic varicosity of a sympathetic nerve terminal. (*A*) Random distribution of synaptic vesicles (○) and calcium channels (●). (*B*) Higher magnification of *A*, showing a random distribution of vesicles in relation to a single open channel.

Heuser and Reese, 1973); additional particles are often found in close juxtaposition to the synaptic vesicles (Heuser et al., 1979).

This paper presents a theoretical investigation of the quantal releases resulting from the opening of a single calcium channel under the three different spatial distributions of vesicles described above. Both the cases of fixed channel open times and random (exponentially distributed) channel open times are considered. The channel is also allowed to have a range of possible positions relative to the vesicles. Equations are derived for the stochastic interaction of the diffusing calcium ions with the vesicle-associated proteins involved in exocytosis and these are solved (numerically) to calculate the probabilities of monoquantal and multiquantal release for each case. The calculations are repeated for a range of values of the calcium channel current and the density of the vesicle distribution. The present model indicates that multiquantal spontaneous release may occur more frequently at varicosities and boutons than at the active zones of motor nerve terminals.

METHODS

Calcium concentration due to stochastic opening of single channels

The presynaptic terminal occupies the region $z > 0$. Calcium channels are situated on the surface $z = 0$, and calcium ions enter from the region $z < 0$ and then diffuse in the region $z > 0$. Let $c(r,t)$ denote the excess calcium concentration at point $\mathbf{r}$, where $\mathbf{r} = (x,y,z)$ denotes a general point in three-dimensional space, at time t after the opening of a calcium channel. Then (Fogelson and Zucker, 1985; Parnas et al., 1989)

$$\frac{\partial c}{\partial t} = \frac{D}{1+B}\nabla^2 c, \tag{1}$$

where D is the diffusion constant for aqueous solution, and B is the ratio of bound to free calcium due to the rapid binding of calcium to a uniformly distributed set of fixed binding sites. Eq. 1 is to be solved subject to the boundary conditions

$$c \to 0 \text{ as } |x|,|y|, \quad \text{and } z \to \infty \tag{2}$$

and

$$D\frac{\partial c}{\partial z} = -f(x,y)g(t) \qquad \text{on } z = O, \tag{3}$$

and the initial condition

$$c(\mathbf{r},0) = 0. \tag{4}$$

The functions $f(x,y)$ and $g(t)$ describe the spatial location and temporal opening, respectively, of a calcium channel in the surface $z = 0$. The channel profile is taken to be Gaussian, so (Parnas et al., 1989)

$$f(x',y') = Af_x(x')f_y(y'), \tag{5}$$

where

$$f_x(x') = \frac{1}{\sqrt{2\pi\sigma}}e^{-(x'-x)^2/2\sigma^2}, \tag{6}$$

and similarly for $f_y(y')$. A and σ are constants giving the amplitude and shape of the profile.

These equations can be solved (e.g., using Green's function techniques; Morse and Feshbach, 1953) to give for the calcium concentration at a distance r from the center of a single channel

$$c(r,t) = \frac{A}{1+B}\frac{2}{\pi^{3/2}} \times \int_0^t \frac{1}{\sqrt{\beta(t-\tau)[\beta(t-\tau)+2\sigma^2]}}e^{-r^2/[\beta(t-\tau)+2\sigma^2]}g(\tau)d\tau, \tag{7}$$

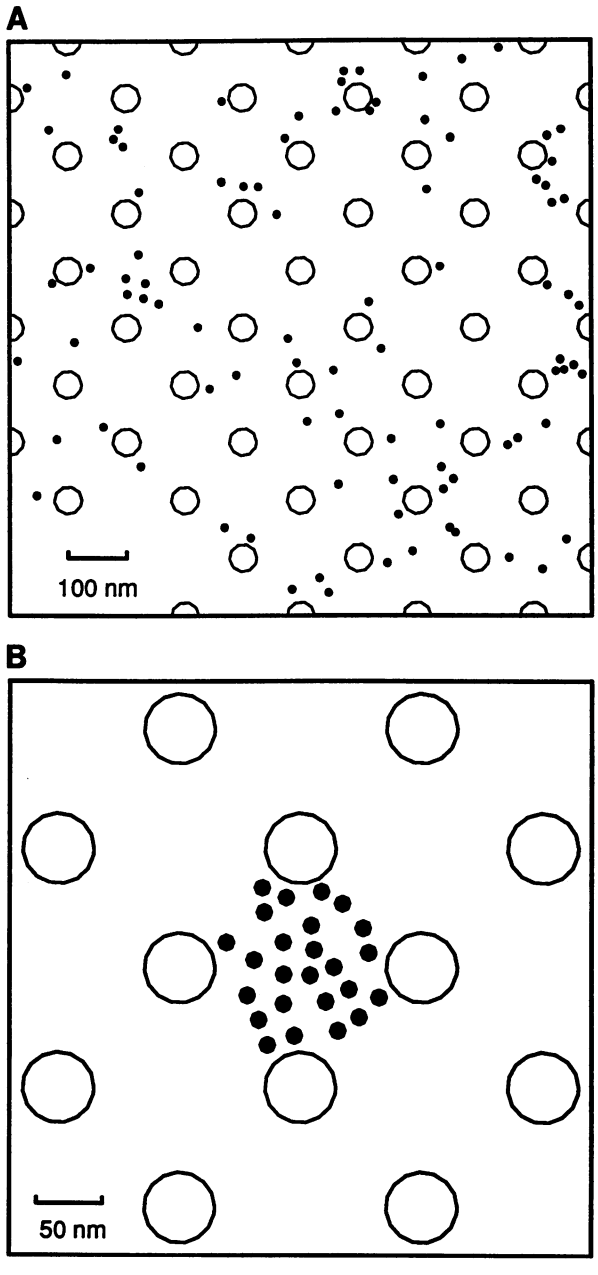

FIGURE 2 Active zone of a synaptic bouton. (*A*) Diamond arrangement of vesicles in a presynaptic grid (○), with random distribution of calcium channels (●). (*B*) Higher magnification of *A*, showing regular vesicle arrangement with a randomly placed open calcium channel; a number of possible positions of the open channel are shown.

where

$$\beta = \frac{4D}{1+B}. \tag{8}$$

If the channel opens at $t = 0$ and closes at $t = t_c$ then the appropriate choice for $g(t)$ is the deterministic step function

$$g(t) = \begin{cases} G & 0 \le t \le t_c, \\ 0 & t > t_c, \end{cases} \tag{9}$$

where G is a constant. The calcium concentration can then be found using numerical integration in Eq .7; in the special case where $\sigma = 0$, Eq. 7 with $g(t)$ given by Eq. 9 can be evaluated explicitly as

$$c(r;t) = \left\{ \begin{array}{ll} \dfrac{AG}{2D\pi r}\left[1 - P\left(\dfrac{1}{2}, \dfrac{r^2}{\beta t}\right)\right], & 0 \le t \le t_c, \\ \dfrac{AG}{2D\pi r}\left[P\left(\dfrac{1}{2}, \dfrac{r^2}{\beta(t-t_c)}\right) - P\left(\dfrac{1}{2}, \dfrac{r^2}{\beta t}\right)\right], & t > t_c, \end{array} \right\} \tag{10}$$

where $P(a, x)$ is the incomplete γ-function (Abramowitz and Stegun, 1965, section 6.5):

$$P(a,x) = \frac{1}{\Gamma(a)} \int_0^x e^{-t} t^{a-1} dt. \tag{11}$$

The product AG is the single channel current, equal to the number of calcium ions passing through a single channel in unit time.

As an example of the use of Eqs. 7 and 10, Fig. 4 *A* shows the calcium concentration at a point 30 nm away from a channel that opens for 0.2 ms. The calcium concentration continues to rise while the channel is open, and then falls to very low values in about a further 1 ms.

More generally, $g(t)$ can be a stochastic step function, such that the channel opens at $t = 0$ and closes at $t = T_c$ where T_c is a random variable. Then $g(t)$ is given by Eq. 9 with t_c replaced by T_c. The closing time T_c is taken to be exponentially distributed with mean $\bar{t}_c = 1/\kappa$ and so has density function

$$f_{T_c}(t) = \kappa e^{-\kappa t}. \tag{12}$$

(See Fig. 5 *A* below for an example of such a distribution.) With this choice of $g(t)$ the calcium concentration as given by Eq. 7 or 10 becomes a random variable, and it is necessary to perform a number of simulations to calculate averages of measurable quantities.

Stochastic binding of calcium to the exocytotic vesicle-protein

It is assumed that several sites on a particular vesicle-associated protein must each bind a calcium ion for exocytosis by a vesicle to be triggered, so secretion does not occur until all such sites are occupied by calcium ions (Südhof and Jahn, 1991). Let $\mu(t)$ be the rate of attachment and $\nu(t)$ be the rate of detachment of calcium ions at a site. Let $P_k(t)$ be the probability that each of k binding sites is occupied by a calcium ion at time t. If there are four such sites (Dodge and Rahamimoff, 1967; Augustine et al., 1987), then $P_4(t)$ is also the probability that a quantum is released by time t. It follows from standard techniques (Feller, 1950, ch. 17) that these probabilities must satisfy the following set of coupled differential equations:

$$\begin{aligned} \frac{dP_0}{dt} &= \nu P_1 - 4\mu P_0, \\ \frac{dP_1}{dt} &= \nu(2P_2 - P_1) + \mu(4P_0 - 3P_1), \\ \frac{dP_2}{dt} &= \nu(3P_3 - 2P_2) + \mu(3P_1 - 2P_2), \\ \frac{dP_3}{dt} &= -3\nu P_3 + \mu(2P_2 - P_3), \\ \frac{dP_4}{dt} &= \mu P_3, \end{aligned} \tag{13}$$

with initial conditions

$$P_0(0) = 1, \qquad P_k(0) = 0, \quad k \ge 1. \tag{14}$$

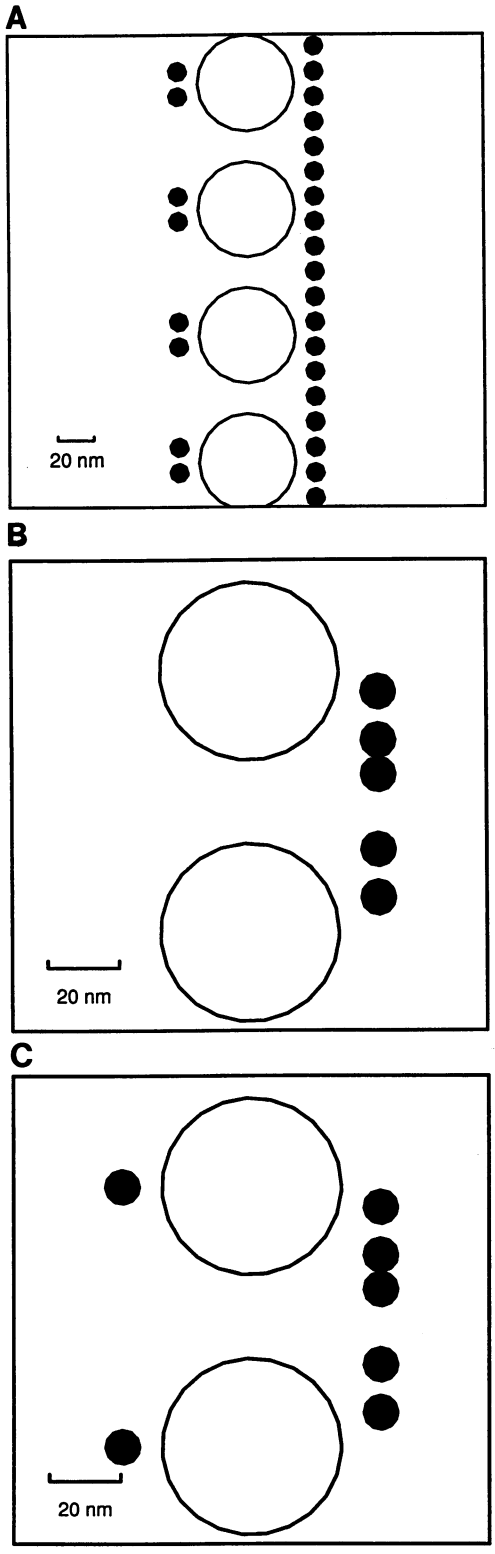

FIGURE 3 Active zone at a motor nerve terminal. (*A*) Single row of calcium channels (○), apposed by a parallel row of synaptic vesicles (●); also shown are two extra channels close to each vesicle. (A second pair of channel-vesicle rows present at a motor nerve terminal are not shown, as they are sufficiently far away to have little effect for spontaneous release.) (*B*) Higher magnification of *A*, showing an open channel situated at random between two vesicles; several possible positions shown. (*C*) As for *B*, but with a typical close channel shown for each vesicle.

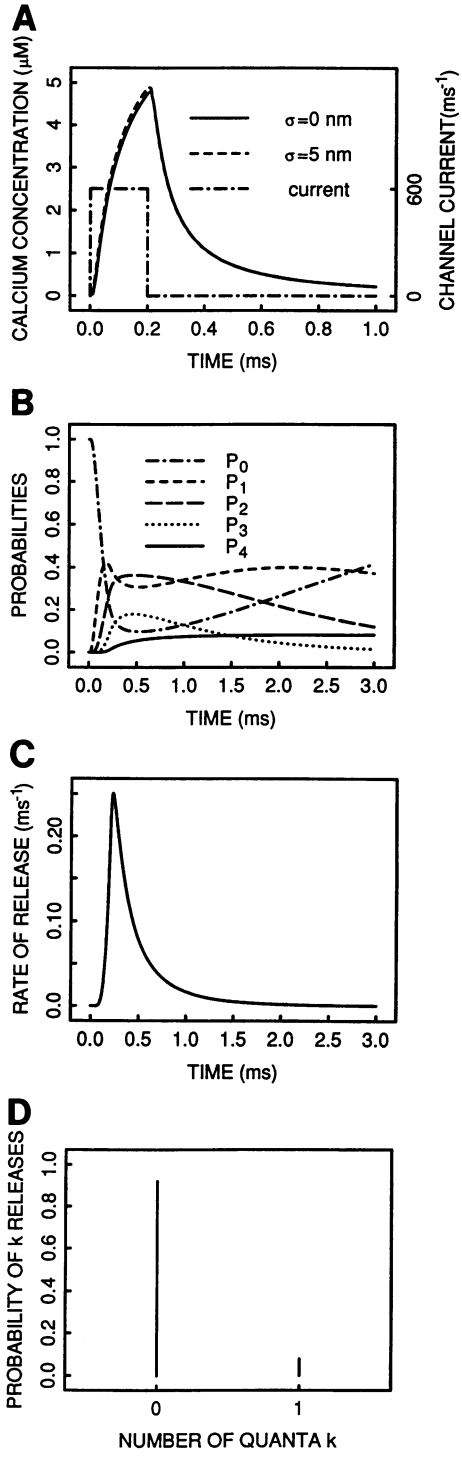

FIGURE 4 Probability of release of a single vesicle 30 nm from a calcium channel open deterministically for 0.2 ms. Other parameter values are as given in Table 1. (*A*) Change in calcium concentration at the vesicle (solution to Eq. 7 or 10). The solid curve is for $\sigma = 0$ and the broken curve for $\sigma = 5$ nm. The more realistic value $\sigma = 2.5$ nm gives a curve that is almost indistinguishable from the solid curve, and has not been shown. The dot-dash curve shows the time course of the channel current, given in ions/ms. (*B*) Probabilities $P_k(t)$ that, given the calcium change in *A*, the vesicle-associated exocytotic protein has bound up to k calcium ions by time t, where $k = 0, 1, 2, 3$, or 4. These probabilities are calculated using Eq. 13. (*C*) Rate (dP_4/dt) of release of a quantum from the vesicle at time t. (*D*) Probability $P(K = k)$ of release of k quanta at long time ($t = 10$ ms). Because there is only one vesicle, $k = 0$ or 1.

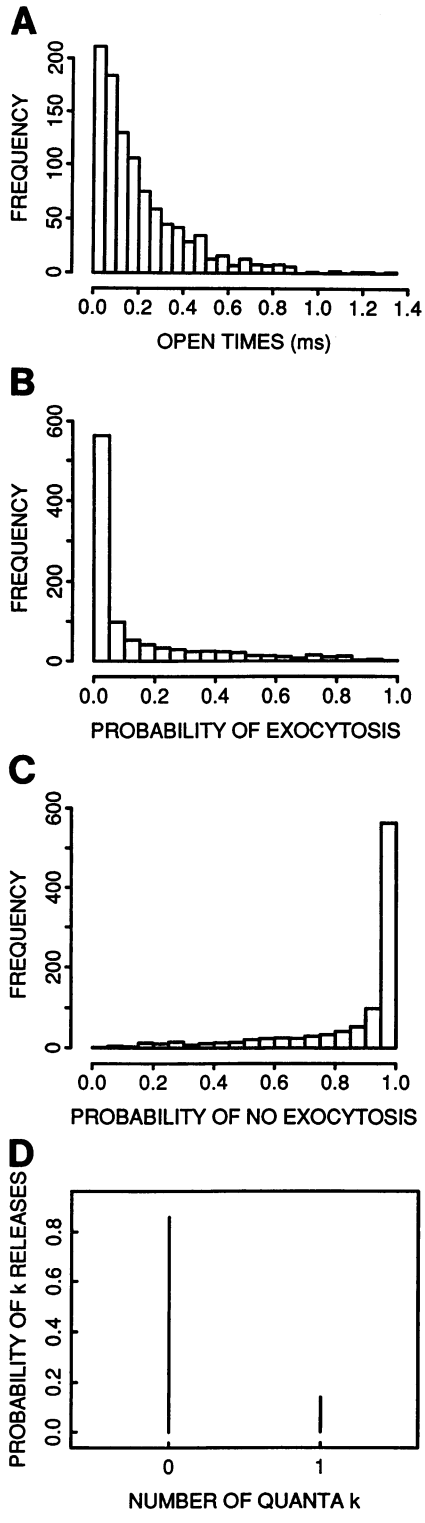

FIGURE 5 Probability of release of a single vesicle 30 nm from a calcium channel that has a stochastic distribution of open times. (*A*) Exponential distribution of open times of the channel, with mean open time of 0.2 ms; 1000 simulations are shown. (*B*) Probability (P_4) that the exocytotic protein of the vesicle has bound four calcium ions at long times (10 ms) for each of the 1000 channel open times in *A*; the frequency is given for each value of P_4 in 0.05 bins. (*C*) the probability that the exocytotic protein of the vesicle does not have four calcium ions at long times (10 ms) for each of the 1000 channel open times in *A*; the frequency is given in 0.05 bins. (*D*) Probability of release of the vesicle.

These equations can also be derived from the kinetic scheme

$$S_0 \underset{\nu}{\overset{4\mu}{\rightleftarrows}} S_1 \underset{2\nu}{\overset{3\mu}{\rightleftarrows}} S_2 \underset{3\nu}{\overset{2\mu}{\rightleftarrows}} S_3 \overset{\mu}{\rightarrow} S_4 \tag{15}$$

where S_i denotes the state with i sites occupied.

To determine the probability $P_4(t)$ that a particular vesicle releases a quantum by time t after the opening of a single calcium channel, the rate of attachment of calcium ions to the binding site of that vesicle has been taken to be proportional to the calcium concentration at the position of the vesicle-associated protein; that is,

$$\mu(t) = k_a c(r,t), \tag{16}$$

where k_a is a constant and $c(r,t)$ is given by Eq. 7 or 10. The rate of detachment of calcium ions is given by

$$\nu(t) = k_d, \tag{17}$$

where k_d is a constant, independent of time.

In the present work, emphasis is placed on the influx and diffusion of calcium ions to the vesicles and the subsequent attachment of these ions to the vesicle-associated protein responsible for allowing exocytosis, as it is in the secretion models of Bennett et al. (1977) and Van der Kloot (1988). If, however, exocytosis is taken as rate limiting as in the models of Parnas et al. (1989) and of Yamada and Zucker (1992), then an extra step may be included in Eq. 13.

Solution of Eq. 13 now gives the probabilities that the vesicle protein responsible for exocytosis has bound from zero up to four calcium ions at its four calcium binding sites at some time t after the opening of the channel. Fig. 4 *B* shows this solution for the case of a single vesicle at a distance of 30 nm from a channel that opens for 0.2 ms (and thus the calcium concentration is given in Fig. 4 *A*). P_4 increases to a value of 0.081 at ~2 ms after the channel opens and remains constant thereafter. The rate of vesicle exocytosis at time t after the opening of the channel is given by dP_4/dt and is shown in Fig 4 *C*; this rate is maximal at 0.23 ms, just after the channel closes. The probability of a failure to release, or of a release, is an immediate consequence of the long-time value of $P_4(t)$ and is shown in Fig. 4 *D*; a release occurs in only ~8% of trials.

Consider again the case above of a single calcium channel at 30 nm from a single vesicle, but with the calcium opening stochastically; the channel opens at $t = 0$ and closes at $t = T_c$, where T_c is exponentially distributed with mean of 0.2 ms as shown in Fig. 5 *a*. Eq. 13 is solved under these conditions to give $P_4(r,t)$ for $r = 30$ nm and $t = 10$ ms, this time being long enough for P_4 to have always reached a constant value. The results for 1000 channel openings are shown in Fig. 5 *B*; on more than 560 occasions the channel opens for such a short time (see Fig. 5 *A*) that the calcium concentration at the vesicle exocytosis protein is so low that there is very little chance of all four binding sites being occupied by calcium ions at any time ($P_4 < 0.05$). It is only for the relatively long open times ($T_c \gtrsim 0.5$ ms) that P_4 is greater than 0.5 (compare Fig. 5 *B* with Fig. 5 *A*). The frequency of the probability that release does not occur over the 1000 channel openings is shown in Fig. 5 *C*, and the frequency of the probability that release does occur is shown in Fig. 5 *B*. The probability of a failure to release, or of a release, is then the average over these frequencies and is given in Fig. 5 *D*; there is now a release on ~14% of occasions.

Release probabilities for various distributions of vesicles and calcium channels at release sites

In general there are two stochastic elements in any calculation: a spatial one, involving the configuration of vesicles and channels, and a temporal one, involving the open times of a calcium channel. The most efficient way of treating this numerically is by using a Monte Carlo simulation with the following steps.

1. A typical configuration of vesicles and channels is generated. Following are the three cases considered.

Case A: random distribution of vesicles and channels

The synaptic vesicles are distributed randomly over the presynaptic membrane with density λ_ν, and calcium channels are also distributed randomly (Fig. 1). This is likely to be the case for sympathetic synaptic varicosities, in which the active zone shows no ordered array of synaptic vesicles in the presynaptic membrane (see Introduction). In the simulation, vesicles are placed at random in a square of side 1 μm such that no overlaps occur (if a vesicle overlaps, it is discarded and the coordinates of its center regenerated). A calcium channel is then placed at random in a central square of side 0.5 μm, again without overlap with any vesicle.

Case B: vesicles on a regular lattice with a random distribution of channels

Vesicles are placed at the nodes of a diamond lattice on the presynaptic membrane, internodal distance $2a$, with calcium channels distributed at random (Fig. 2), as is appropriate for synaptic boutons (see Introduction). Thus once a is given the vesicles are fixed and it is only necessary to generate the position of the channel that will open, again avoiding overlaps with the vesicles. Because of symmetry, channel positions in only one quadrant of a diamond need be considered.

Case C: vesicles and channels on lines

In this case vesicles are constrained along lines and calcium channels along parallel lines (Fig. 3), as occurs at the active zones of release sites in somatic motor nerve terminals (see Introduction). Once the positions of the lines and the vesicle separation has been specified the only variable is the position of the open channel on its line, and this is taken to be at a random position relative to two vesicles (Fig. 3 *B*). There is also the possibility of extra channels close to individual vesicles, as show in Fig. 3, *A* and *C*.

In all three cases the result of this first step is a set of distances $r_1, r_2 \ldots, r_n$ from the channel to the n closest vesicles. A maximum value of $n = 8$ was found to be sufficient for all calculations in this paper.

2. The open time t_c of the channel is now chosen. It will either be deterministic, in which case the same value is used in all the simulations; or stochastic, in which case a different value is chosen (from an exponential distribution) for each simulation.

3. The set of coupled differential equations in Eq. 13 is now solved (numerically) for $p_i(t) = P_4(r_i,t)$, $i = 1, \ldots, n$ where the distance r_i has been included in the argument of P_4 to emphasize that the release probability depends on the distance of a vesicle from a calcium channel. The result of this step is thus a set of release probabilities $p_1(t), p_2(t), \ldots, p_n(t)$ for the n closest vesicles.

4. Let $K(t)$ be a random variable equal to the number of quanta released by time t after the channel opens. Then the probability of k releases by time t is given by

$$P(K(t) = k) = \text{coefficient of } s^k \text{ in } \prod_{i=1}^{n} (p_i(t)s + q_i(t)), \qquad k = 0,1, \ldots, n, \tag{18}$$

where $q_i(t) = 1 - p_i(t)$. Usually the quantity of interest is the probability $P(K = k)$ that k releases occur, given by

$$P(K = k) = \lim_{t\to\infty} P(K(t)=k). \tag{19}$$

In practice $P(K(t) = k)$ reaches its final value in a few ms. For channel openings of up to 2 ms the limiting value was reached well before the 10 ms used in the calculations below.

5. The above probability is conditional on the spatial configuration and on the channel open time, i.e., it is really $P(K = k|R_i = r_i, T_c = t_c)$ where R_i stands for the random distances from the channel to the vesicles and T_c is the random open time. The unconditional probability $P(K = k)$ is now found by repeating the whole simulation a number of times (typically, 1000) and taking the average.

6. Because only actual releases are observed, the quantity of real interest is the conditional probability $P(K = k|K \geq 1)$ that $k = 1, 2, \ldots, n$ releases occur given that at least one release occurs, and this is given by

$$P(K = k \mid K \geq 1) = \frac{P(K = k)}{1 - P(K = 0)}. \tag{20}$$

In Case A it is possible to proceed further analytically if the finite size of the vesicles and channel is neglected. The probability that each of k vesicles has released a quantum by time t is given by the Poisson distribution:

$$P(K(t) = k) = \frac{[\pi\lambda_\nu q(t)]^k}{k!} e^{-\pi\lambda_\nu q(t)}, \quad k = 0,1, \ldots \tag{21}$$

where

$$q(t) = \int_0^\infty P_4(r,t)2rdr, \tag{22}$$

and $P_4(r,t) \equiv P_4(t)$ is found by solving Eq. 13. The derivation of Eq. 21 is given in the Appendix. This formula provides a useful check on the Monte Carlo method; even for vesicles and channel of finite size it is quite accurate at low densities, but becomes increasingly inaccurate as the density increases. In all calculations reported below the Monte Carlo method has been used.

General considerations

The present model does not incorporate the pumping of calcium out of the terminal or the interaction of calcium with buffers. Calculations including an expression for the pump in Eq. 1, and using values for pumping suggested by Fogelson and Zucker (1985), indicated that this is likely to have negligible effects on the present results. However, failure to account for the kinetics of interaction between calcium and its buffers as done by Yamada and Zucker (1992) as well as by Simon and Llinás (1985) might have more serious consequences for quantal secretion. In the present work, diffusion is slowed from its value in aqueous solution by very rapid binding to uniformly distributed fixed binding sites, using a diffusion constant reduced by an amount B (for discussion of appropriate values for B see Augustine et al., 1987). The stochastic interaction between calcium and both high and low affinity buffers will be addressed in future work, as this greatly complicates a probabilistic analysis of the kind presented here. One very important objection to some previous models is the failure to account for the high temperature dependence of secretion as a consequence of taking secretion as proportional to a power of the calcium concentration (Fogelson and Zucker, 1985). This can be met by incorporating temperature dependence into the stochastic processes involving the vesicle-associated exocytosis protein (see also Yamada and Zucker, 1992).

The power relationship between intracellular calcium and transmitter release has been taken as $n = 4$ at the different active zone types investigated. Experiments in which the extracellular calcium concentration is changed and quantal release measured have given an $n = 4$ for mammalian sympathetic varicosities (Macleod et al., 1994) and amphibian neuromuscular junctions (Dodge and Rahamimoff, 1967). Sympathetic preganglionic nerve terminals, consisting of clusters of synaptic boutons (Streichert and Sargent, 1989), show a two- to threefold power relationship (Bennett et al., 1976). There is more direct evidence for cooperativity of about three calcium ions in secretion at the squid giant synapse, where it has been shown that the postsynaptic current varies as the third power of the presynaptic calcium current (Smith èt al., 1985; Augustine et al., 1985), with some synapses showing a power as high as four in an external calcium concentration of 3 mM (Augustine and Charlton, 1986). There has been

considerable discussion of the extent to which the spatial distribution of open calcium channels, together with their local domains of high calcium concentration, determine the power relation between presynaptic calcium currents and secretion (Zucker and Fogelson, 1986). It has recently been argued that there is a cooperative triggering of release within the influence of a single domain, at least at the squid giant synapse, indicating multiple binding sites for calcium on the vesicle-associated protein controlling exocytosis (Augustine et al., 1991).

Although it is clear that a power relationship exists between calcium and evoked transmitter release, it is not clear whether this is likely to hold for spontaneous release, and if so what types of calcium channel are likely to be involved. The frequency of spontaneous release at the amphibian and mammalian neuromuscular junctions shows a dependency on the external calcium concentration (Rotschenker and Rahamimoff, 1970; Hubbard et al., 1968), as it does for amphibian and mammalian preganglionic boutons on autonomic neurons (Dennis et al., 1971; Bornstein, 1981). The ω-conotoxin GVIA-sensitive calcium channel (N-type; Fox et al., 1987) determines at least part of the spontaneous quantal release at the amphibian neuromuscular junction, as blocking it reduces the frequency by half (Grinnell and Pawson, 1989); other unidentified calcium channels (either voltage-sensitive or insensitive) are implicated also, as reducing the external calcium to very low values reduces the spontaneous frequency by 90% (Grinnell and Pawson, 1989). However, it is possible that the intraterminal release of calcium from calcium stores also contributes to spontaneous release (Berridge, 1992; Melamed et al., 1993; Cohen et al., 1981). The contribution of such sources of calcium is not considered here.

Although there is little evidence concerning the calcium channel types involved in spontaneous quantal secretion at different synapses, there is for evoked secretion. Amphibian neuromuscular transmission is blocked by ω-conotoxin GVIA (Kerr and Yoshikami, 1984), indicating a role for N-type calcium channels (Fox et al., 1987; but see Ellinor et al., 1993), whereas mammalian neuromuscular transmission is blocked by ω-Agatoxin-IVA (Llinás et al., 1992) indicating a role for P-type calcium channels (Usowicz et al., 1992). Sympathetic neuromuscular transmission and synaptic transmission are blocked by ω-conotoxin GVIA (de Luca et al., 1990; Plummer et al., 1989). However, synaptic boutons in the central nervous system show differential sensitivity to blockade of transmitter release by different neurotoxins, depending on the boutons considered. Thus glutamate release in the striatum and hippocampus is mostly under the control of P-type channels (Turner et al., 1993; Luebke et al., 1993), which is the predominant class of calcium channel in these structures (Mintz et al., 1992), whereas the release of GABA is mostly under the control of N-type channels (Horne and Kemp, 1991). The role of ω-conotoxin GVIA and ω-Agatoxin-IVA-resistant channels in transmitter release from central boutons is yet to be elucidated (Turner et al., 1993). The active zones considered in the present work belonged to mammalian sympathetic neuromuscular varicosities (Fig. 1), amphibian neuromuscular release sites (Fig. 3), and mammalian preganglionic boutons (Fig. 2), all of which produce an evoked secretion dependent on N-type calcium channels. Characteristics of the open times of these channels have therefore been used in the stochastic modeling. In the absence of these characteristics for the P-type channels, we have also used the N-type channel open times for modeling central boutons. This channel type shows three open probability modes. As the voltage dependence of these open times has now been determined for each mode it is possible to obtain quantitative estimates for the channel open times at the resting membrane potential (Delcour et al., 1993).

RESULTS

Numerical values of parameters

The numerical values of the parameters used in the calculations are listed in Table 1. The channel current is the product of a spatial amplitude A and a temporal amplitude G. Parnas et al. (1989) give a value of 550 calcium ions per ms, which has been rounded to 600 in Table 1. This value is used in all calculations except for those shown in Fig. 9, where the effect of varying the calcium channel current is investigated. If the channels are taken to be particles of 10 nm diameter, then a reasonable choice for the channel spatial profile parameter σ would be 2.5 nm. However, even in the extreme case where the channel and vesicle touch, there is almost no difference in the calcium concentration at the center of the vesicle for $\sigma = 2.5$ nm and $\sigma = 0$ (see Fig. 4 *A*). Hence $\sigma = 0$ has been used, as one significant advantage is that the analytic formula Eq. 10 can be used instead of the integral Eq. 7 with considerable saving in computational time.

The channel open time is a random variable T_c, which is taken to be exponentially distributed with mean 0.2 ms; this is obtained by extrapolating to −60 mV the data of Delcour et al. (1993) for low-p_o N-type channels (see their Fig. 13 *B*). Sometimes calculations are done with a deterministic opening time of 0.2 ms, but these are either for simple illustration or else as a contrast to the stochastic case; as will be emphasized below, release probabilities calculated on the basis of deterministic open times can be very misleading.

The calcium attachment rate coefficient k_a has been set at 0.6 μM^{-1} ms^{-1}, because this seems to give the best illustration of differences caused by various geometries. Because k_a always appears in the combination $k_a AG$ the effect of varying k_a is the same as that of varying the channel current $A \times G$, and this will be investigated in Fig. 9. The detachment rate k_d has been set at 0.5; the effect of varying

TABLE 1 Values of the parameters used in the numerical calculations

Quantity	Symbol	Value	Reference
Calcium diffusion coefficient	D	0.6 μm^2 ms^{-1}	Fogelson and Zucker (1985)
Bound to free calcium ratio	B	100	Augustine et al. (1987)
Single channel current	$A \times G$	600 ms^{-1}	(See text)
Channel spatial profile parameter	σ	0	(See text)
Random channel open time	T_c	mean = 0.2 ms	Delcour et al. (1993)
Calcium attachment rate coefficient	k_a	0.6 μM^{-1} ms^{-1}	(See text)
Calcium detachment rate coefficient	k_d	0.5 ms^{-1}	(See text)
Calcium channel diameter		10 nm	Heuser et al. (1979) Pumplin et al. (1981)
Vesicle diameter		50 nm	Heuser et al. (1979) Akert et al. (1971)

this can be compensated for by an appropriate change in k_a, so a different choice for k_d simply leads to another choice for k_a with very little change in the overall results. These values for k_a and k_d give relatively high affinity bindings (see also Parnas et al., 1989), whereas recent results suggest that the fast phase of evoked quantal release is likely to involve a lower affinity binding (see Heidelberger et al., 1994; Heinemann et al., 1994). It seems, however, that spontaneous release might be more closely related to the slow phase of evoked quantal release (Goda and Stevens, 1994), which is likely to involve a high affinity binding. Some results for a lower-affinity binding are given in the section on the effect of varying the affinity of binding on the probability of multiquantal release, below.

Determination of the probability that *k* vesicles release quanta on opening of a calcium channel

Random distribution of vesicles at active zones (sympathetic varicosities)

Consider the case of vesicles randomly distributed in an active zone with density $\lambda_v = 250\ \mu m^{-2}$ and deterministic opening of a calcium channel within the zone, with open time 0.2 ms. The simulation method outlined earlier allows calculation of the probabilities $P(K = k|K > 0)$ of k quantal releases conditional on not being able to count failures to secrete. Fig. 6 *A* shows that in this case only ~12.6% of all spontaneous secretions will involve two vesicles releasing quanta; releases of three or more quanta are negligible, and the variance of the distribution is very small compared with the mean.

Consider now the case of vesicles randomly distributed in an active zone with density $\lambda_v = 250\ \mu m^{-2}$ and stochastic opening of a calcium channel within the zone, the open time being exponentially distributed with mean 0.2 ms. Averaging over 1000 channel openings, with open times taken from this exponential distribution, leads to the conditional probabilities shown in Fig. 6 *B*. Now ~32% of releases are multiquantal: ~21.5% double, ~7.5% triple and ~2.5% quadruple; the variance of the distribution has therefore increased greatly in this stochastic case, but is still less than the mean. There is thus a dramatic increase in the number of multiquantal releases when the channel open time is allowed to be stochastic. This is a direct consequence of the exponential distribution allowing an appreciable fraction of very long open times (Fig. 5 *A*).

Vesicles distributed on a grid in active zones (synaptic boutons)

In this case, vesicles are distributed on a diamond-shaped grid with dimensions shown in Fig. 2 *B*, giving a vesicle density of 200 μm^{-2}. The procedure outlined above in Methods allows calculation of the probabilities $P(K = k|K > 0)$ of k quantal releases conditional on not being able to count failures to secrete, for the case of stochastic opening of a calcium channel with exponentially distributed open times of mean 0.2 ms. Averaging over 1000 channels, any one of which can occupy a random position in the diamond grid as shown in Fig. 2 *B*, gives the results shown in Fig. 7. About 29% of releases are multiquantal, which is similar to the case for random distribution of vesicles at the active zone (compare Fig. 7 with Fig. 6 *B*). The exponential

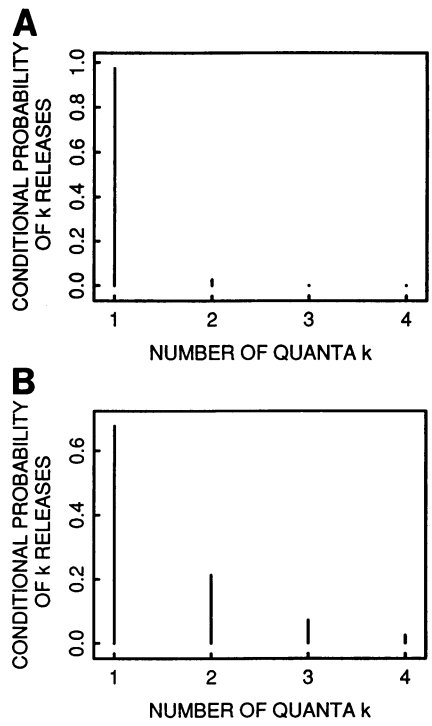

FIGURE 6 Probability of release of different numbers k of vesicles placed at random in an active zone (varicosity case) with density $\lambda_v = 250\ \mu m^{-2}$, upon the opening of a single calcium channel (Fig. 1 *B*). (*A*) Probability $P(K = k|K > 0)$ of release conditional on not counting failures for deterministic opening (0.2 ms) of the single channel. (*B*) $P(K = k|K > 0)$ conditional on not counting failures for stochastic opening (exponential with mean 0.2 ms) of the single channel.

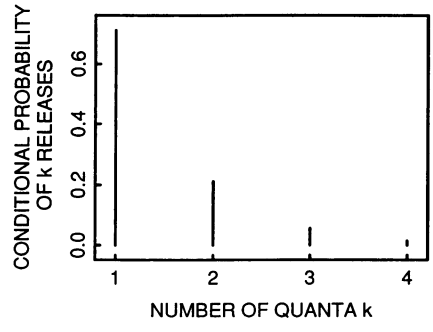

FIGURE 7 Probability of release of different numbers k of vesicles on a rectangular grid in the active zone (bouton case) with density $\lambda_v = 200\ \mu m^{-2}$, when the single channel that opens can take a random position relative to the vesicles (Fig. 2 *B*). The graph shows $P(K = k|K > 0)$ for random channel open times (exponential with mean 0.2 ms).

distribution of open times was chosen to have a mean of 0.2 ms, as for N-type calcium channels, although it is known that P- and Q-type calcium channels play a prominent role in calcium-dependent transmitter release from boutons (Turner et al., 1993; Wheeler et al., 1994). However, there are not as yet published records on their average open times; if these are longer than 0.2 ms then the extent of multiquantal release will be increased further. Another possibility that would increase multiquantal release is that the dimension of the diamond lattice is smaller, allowing the vesicle density at boutons to approach that assumed for varicosities (namely, 250 μm^{-2} rather than 200 μm^{-2}).

Vesicles and calcium channels distributed on lines in active zones (motor endplates)

In this case, vesicles are distributed on a line with dimensions shown in Fig. 3 *A*; the center-to-center distance between vesicles is 70 nm (Heuser et al., 1979), giving a vesicle density of 14.3 μm^{-1}. If the N-type channels at an amphibian endplate active zone open with mean time of 0.2 ms, and the open channels occur randomly at any point along a line parallel to that on which the vesicles are positioned (Fig. 3 *B*), then averaging over 1000 openings gives the conditional probabilities of k quantal releases as shown in Fig. 8 *A*. In this case, <10% of releases are multiquantal. If an extra channel is associated with each vesicle (Fig. 3 *C*; see Heuser et al., 1979) then multiquantal release is reduced to ~4% (Fig. 8 *B*), a condition that occurs experimentally (see del Castillo and Katz, 1954).

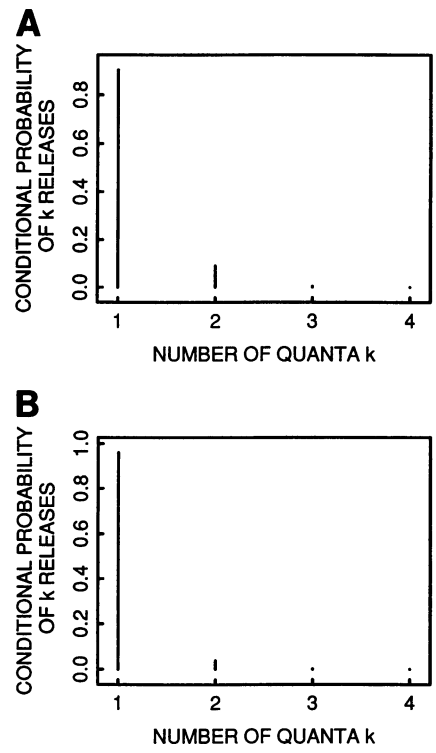

FIGURE 8 Probability of release of different numbers k of vesicles on a line in the active zone (motor terminal case) with vesicle centers 70 nm apart, when the single channel that opens can take a random position between two vesicles (Fig. 3 *B*). The graphs show $P(K = k|K > 0)$ for random channel open times (exponential with mean 0.2 ms). (*A*) all the channels lie on a line parallel to the line of centers of the vesicles and 35 nm distant. (*B*) An additional channel is associated with each vesicle (Fig. 3 *C*); this channel is taken to be 35 nm from the vesicle center and effects only that vesicle.

Factors determining multiquantal spontaneous secretion at active zones

As mentioned in the Introduction, there is evidence for multiquantal spontaneous secretions from the active zones of mature sympathetic varicosities, developing boutons and developing motor endplates. Given the geometrical relations between vesicles and calcium channels within an active zone, there are several properties that primarily govern multiquantal secretion: these are the current ($A \times G$) and opening times (T_c) of the calcium channels, the density of vesicles (λ_v) in the active zone, and the rate of reaction between the calcium ions and the vesicle fusion protein. In this section the effects of varying these parameters on the probability of multiquantal releases is explored.

Effect of increasing calcium channel open times and current on the probability of multiquantal releases

The effect of increasing the single channel current ($A \times G$) on the extent of multiquantal release has been calculated for each of the main active zone types encountered. These are active zones with randomly placed vesicles (Fig. 1), with vesicles on a diamond grid and opening of channels at random positions (Fig. 2), and finally with vesicles on a line and channels opening at random positions along a parallel line (Fig. 3). Fig. 9, *A–C*, shows the dependence of the proportion of multiquantal releases on the channel current for each of these cases; respectively, for the condition of a random placement of vesicles with density 250 μm^{-2} in the case of sympathetic varicosities, a diamond grid of vesicles with density 200 μm^{-2} for boutons, and a line of vesicles spaced 70 nm apart for active zones of endplates. Results are shown for both deterministic (0.2 ms) and random (exponential, mean = 0.2 ms) channel open times. In general random open times give a greater fraction of multiquantal releases, except at very high channel currents where the reverse can occur (Fig. 9 *A*). This crossover occurs because at low currents open times >0.2 ms are required if more than one vesicle is to release transmitter, and this occurs only in the random case; at high currents an open time of 0.2 ms is sufficient to ensure that all close vesicles release a quantum, whereas in the random case there will be a proportion of shorter times that give at most one release.

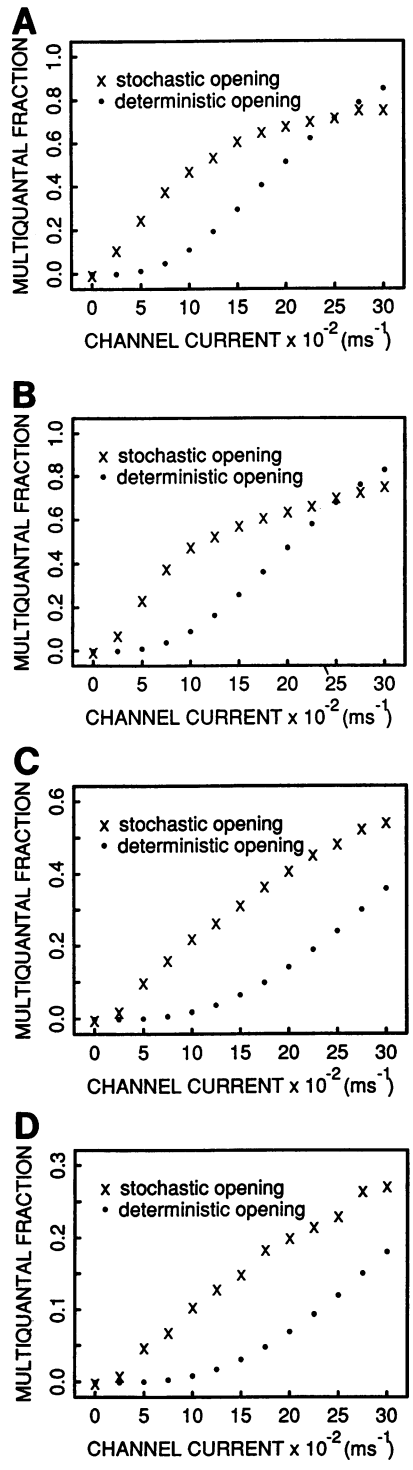

FIGURE 9 Effect of changes in channel current on the probability of multiquantal secretion. The abcissa gives the channel current (in hundreds of ions per ms), and the ordinate gives the fraction of all releases that are multiquantal. The points show the results for deterministic channel open times (0.2 ms), and the crosses for stochastic open times (exponential with mean 0.2 ms). (*A*) Active zone with random vesicles at density λ_v = 250 μm^{-2} (Fig. 1 *B*). (*B*) Active zone with vesicles on a synaptic grid with density λ_v = 200 μm^{-2}, and random position of open channel (Fig. 2 *B*). (*C*) Active zone with vesicles on a line with centers 70 nm apart, and random position of open channel (Fig. 3 *B*). (*D*) Active zone with vesicles on a line with centers 70 nm apart, and random position of open channel plus extra close channel (Fig. 3 *C*).

The multiquantal release increases with channel current in all cases, as expected. However, this increase is greater for spatially random vesicles (Fig. 9 *A*) and for vesicles on a grid (Fig. 9 *B*) than for vesicles on a line (Fig. 9 *C*). An increase in channel current increases the proportion of multiquantal releases for the spatially random and grid cases over the other case (Fig. 9). For a current of 1000 ms^{-1} and stochastic open time with mean 0.2 ms the number of multiquantal releases will be 48%, 48%, and 22% for each of the three active zone types (random, grid, and line) respectively. Incorporation of the extra channel per vesicle for the last case reduces this to 10.5% (Fig. 9 *D*).

Effect of increasing vesicle density on the probability of multiquantal releases

The extent of multiquantal release was determined for the three active zone types when the vesicle density (λ_v) was increased. Fig. 10 shows that for a particular channel current the multiquantal release is much the same at each value of λ_v for the random vesicle case as for the case of vesicles on a grid (compare Fig. 10, *A* and *B*). At densities <100 vesicles per μm^2 the expected multiquantal release is <15% in both cases (Fig. 10, *A* and *B*). For vesicles on a line, multiquantal release does not reach 10% until the high density of 14 vesicles per μm is reached (Fig. 10 *C*); at 20 vesicles per μm, when adjacent vesicles are touching, the multiquantal release is still only ~20%. Incorporation of the extra channel per vesicle reduces multiquantal release substantially (Fig. 10 *D*), so that 10% is only reached when the vesicles touch.

Effect of varying the affinity of binding on the probability of multiquantal release

It is not clear at this time whether the calcium attachment and detachment rate coefficients k_a and k_d for spontaneous quantal release are best taken as those for the fast component of evoked release (with a low affinity k_d of about 20 ms^{-1}) or for the slow component of evoked release (with a higher affinity). We have used the latter interpretation in which the values for k_d and k_aAG are similar to those of Parnas et al. (1989), but explore here the results if low affinity binding is used. In this case a k_d of 20 ms^{-1} may be used in conjunction with a k_a of 0.6 μM^{-1} ms^{-1} as before but with an increase in the single channel current AG from 600 ms^{-1} (used by Parnas et al., 1989) to 1800 ms^{-1} (determined from the recent data of Delcour et al., 1993, for the N-type calcium channel in the low-p_o mode, and allowing for a ratio of calcium versus barium current through these channels of about one-half; see Lux and Brown, 1984). This single channel current of 1800 ms^{-1} is close to the value of 1640 ms^{-1} used by Zucker and Fogelson (1986) in their calculations.

Using the decreased affinity (k_d = 20 ms^{-1}) and increased calcium current (1800 ms^{-1}), the extent of multiquantal spontaneous release for the case of random vesicle

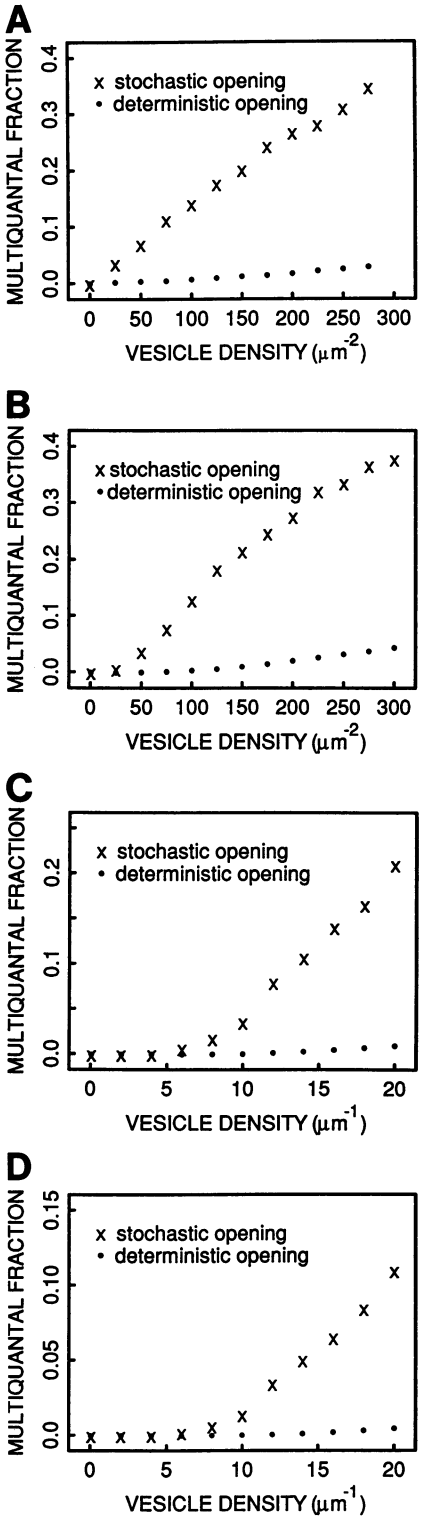

FIGURE 10 Effect of changes in vesicle density on the probability of multiquantal secretion at a fixed channel current of 600 ms^{-1}. The abcissa gives the vesicle density and the ordinate gives the fraction of all releases that are multiquantal. The points show the results for deterministic channel open times (0.2 ms), and the crosses for stochastic open times (exponential with mean 0.2 ms). (*A*) Active zone with random vesicles (Fig. 1 *B*). (*B*) Active zone with vesicles on a synaptic grid and random position of open channel (Fig. 2 *B*). (*C*) Active zone with vesicles on a line and random position of open channel (Fig. 3 *B*). (*D*) Active zone with vesicles on a line and random position of open channel plus extra close channel (Fig. 3 *C*).

placement in the active zone was 11% of all releases, compared with 32% for the high affinity case (see Fig. 6 *B*). The extent of multiquantal spontaneous release for the case of muscles on a line in the active zone was 1.5% of all releases, compared with 4% for the high affinity case (see Fig. 8 *B*). Thus the extent of multiquantal release is reduced about threefold for both active zone structures for the low affinity case. Active zones of motor nerve terminals continue to have a much lower rate of multiquantal release compared with active zones of varicosities.

Comparison between experimental and theoretical spontaneous quantal release distributions at different active zone types

Sympathetic varicosities

At the present time, spontaneous quantal releases have only been recorded directly from individual active zones of sympathetic varicosities (Bennett, 1993, 1994). These show amplitude-frequency histograms that contain multiquantal releases. The percentage of multiquantal responses varies between about 10 and 25% of the releases (Bennett, 1994). This is the result to be expected from the random vesicle distribution model if the channel current is 600 ms^{-1}, the channel open time is stochastic with mean 0.2 ms, and the vesicle density varies between 75 μm^{-2} and 175 μm^{-2} (Fig. 10 *A*).

Synaptic boutons

No recordings have been made of spontaneous quantal secretions from synaptic boutons directly. However, Bekkers et al. (1990) have determined amplitude-frequency distributions of spontaneous quantal secretions from single boutons in hypertonic solutions, recorded from the neuron soma in tissue culture; these very likely contain multiquantal releases. Edwards et al. (1990) have determined amplitude-frequency histograms for spontaneous quantal releases from inhibitory synaptic boutons on granule cells in the immature (17–21-day-old) rat hippocampus; these also contain releases which might be interpreted as multiquantal (their Fig. 13 *B* shows ~50% multiquantal releases). Such apparent multiquantal spontaneous releases are not confined to inhibitory synapses, as they have also been observed at excitatory synapses of mossy fibers on cerebellar granule cells in immature (11–17-day-old) rat cerebellum (Silver et al., 1992), in which an average of 25% of the releases are multiquantal. More recently, multiquantal spontaneous release has been observed at excitatory synapses formed by optic nerve terminals on lateral geniculate neurons; ~20% of the releases are multiquantal, including double and triple releases (Paulsen and Heggelund, 1994). It is known that the active zone of central synaptic boutons does not reach a mature state until postnatal day 30 in the rat (Markus et al., 1987), a time much later than that at which electrophysical

studies are made. The active zone model incorporating a random distribution of channels and vesicles (Fig. 1) may be more appropriate to account for multimodal distributions at the central synapses studied so far, if these multiquantal releases can be interpreted as occurring at a single bouton. This caveat is raised as recordings have recently been made of spontaneous quantal release from single boutons at hippocampal pyramidal neurons, for which there was little evidence of multiquantal release (Gulyas et al., 1993). Furthermore, it may be that there is more than one active zone in those mature boutons for which there is evidence for multiquantal release (for a review of this possibility, see Korn et al., 1994).

The synaptic boutons on autonomic ganglia give rise to spontaneous quantal secretions recorded with an intracellular electrode that do not in general have amplitude-frequency histograms that can be described by a Gaussian distribution (Blackman et al., 1963; Blackman and Purves, 1969). The histograms are often better fitted by a gamma-distribution (McLachlan, 1975; Bennett et al., 1976). Bornstein (1981) shows ~30% multiquantal releases for an autonomic ganglion. A channel current of 600 ms^{-1} gives about 25% multiquantal releases at sympathetic varicosities (Fig. 9 *A*), which also use N-type calcium channels in quantal secretion. About this proportion of multiquanta have been observed at these varicosities (Bennett, 1995).

Motor endplates

Fatt and Katz (1952) noted in the first intracellular recording of spontaneous release at the amphibian motor endplate that the amplitude-frequency histogram of spontaneous potentials was well fitted by a Gaussian distribution, but that a few double quantal releases (i.e., around twice the mean of the Gaussian) could be observed. These were attributed to near coincident and independent release of quanta from different active zones. Although there has been much research on subquantal releases (i.e., releases of much smaller amounts of transmitter than contained in a quantum as defined by the Gaussian; see Kriebel et al., 1982; Bennett, 1995), there is little evidence for multiquantal releases at the endplate. What conditions might pertain at these active zones, which restrict spontaneous release to single vesicles? It is known that N-type calcium channels control calcium influx responsible for secretions at the amphibian endplate, and this restricts the mean open time of the channel to ~0.2 ms. If λ_v is ~14 μm^{-1} (i.e., sufficient to give a vesicle density on the line such that each vesicle is separated from its neighbors by a single space slightly less than half the diameter of one vesicle), then Fig. 9 *D* shows that the channel current must be no greater than 500 ms^{-1} for multiquantal release to be <5% of all quantal releases.

Developing amphibian motor endplates do not possess Gaussian distributions of spontaneous potentials (Kriebel and Gross, 1974; Bennett and Pettigrew, 1975). Shortly after formation of the motor nerve terminal, before the active zones have become organized (Heuser and Reese, 1973; Ko, 1985), multiquantal releases are frequent (Bennett and Pettigrew, 1975). They are also frequent at newly cultured motor nerve synapses (Fig. 13 *A*, Lo et al., 1991). The model involving random distribution of vesicles (Fig. 1) could account for this multiquantal release.

Kriebel and his colleagues (see, e.g., Kriebel and Gross, 1974; Erxleben and Kriebel, 1988; Vautrin and Kriebel, 1991) have presented extensive evidence for the Gaussian distribution of spontaneous potentials at motor endplates possessing a subunit structure. Furthermore, they identified a small positively skewed distribution of spontaneous potentials, with a subunit structure, in addition to the Gaussian distribution. Although the present model does not predict this subunit composition, work in progress indicates that it could arise from stochastic events involved in vesicle exocytosis.

CONCLUSION

The theory for spontaneous quantal secretion developed here may be compared with existing theories for evoked quantal secretion at the squid giant synapse and the amphibian neuromuscular junction. These use a fixed set of open calcium channels in a particular spatial array within an active zone (Fogelson and Zucker, 1985; Zucker and Fogelson, 1986; Parnas et al., 1989; Yamada and Zucker, 1992) or solve deterministic kinetic equations governing channel openings (Llinás et al., 1981a). In the present theory both the opening of a channel and its location within an active zone are stochastic. Previous theories also considered that quantal secretion was either proportional to a power of the calcium concentration at the vesicles (Fogelson and Zucker, 1985) or that it was governed by deterministic kinetic equations involving the concentration of calcium ions and the concentration of a vesicle-associated protein required for exocytosis (Llinás et al., 1981b; Parnas et al., 1989; Yamada and Zucker, 1992). The introduction of techniques to describe what are essentially stochastic events in the calcium-activated secretion process has allowed for a probabilistic description of spontaneous quantal secretion as evidenced in the predicted amplitude-frequency distributions. The present stochastic model tends to give predictions for the level of multiquantal release that are higher than those recorded, even given the caveats concerning whether the recordings are from single active zones or not. This may point to the future necessity of considering whether a refractory system exists within single active zones that restricts the level of multiquantal spontaneous release (Triller and Korn, 1982).

APPENDIX

Derivation of Eq. 21

Let the single open calcium channel be at the origin and suppose it is surrounded by a disc of radius ρ containing N_ρ vesicles placed at random.

(Eventually, ρ will be allowed to go to infinity). Then the distance of a vesicle from the channel is a random variable R with density function

$$f_R(r) = \frac{2r}{\rho^2}, \qquad 0 \le r \le \rho.$$

From Eq. 13, the probability that a vesicle at distance r releases a quantum by time t is $P_4(r,t) \equiv P_4(t)$, so the expected probability of release at a randomly chosen vesicle in the disc is

$$p_\rho(t) = \int_0^\rho P_4(r,t)\,\frac{2r}{\rho^2}\,dr.$$

The conditional probability of k releases given n vesicles inside the disc is given by the binomial distribution

$$P(K(t) = k|N_\rho = n) = \binom{n}{k}[p_\rho(t)]^k[1 - p_\rho(t)]^{n-k}. \quad (23)$$

(Note that it is permissible to use the binomial distribution here because the distances to the vesicles have been treated as independent identically distributed random variables.) The unconditional probability is therefore

$$P(K(t) = k) = \sum_{n=k}^{\infty} P(K(t) = k|N_\rho = n)P(N_\rho = n). \quad (24)$$

Now N_ρ obeys a Poisson distribution, with average $\pi\rho^2\lambda_\nu$, so

$$P(N_\rho = n) = e^{-\pi\rho^2\lambda_\nu}\frac{(\pi\rho^2\lambda_\nu)^n}{n!}, \qquad n = 0,1,2,\ldots \quad (25)$$

Using Eqs. 23 and 25 in Eq. 24 leads to

$$P(K(t) = k) = e^{-p_\rho(t)\pi\rho^2\lambda_\nu}\frac{[p_\rho(t)\pi\rho^2\lambda_\nu]^k}{k!}.$$

This should become independent of ρ for ρ large, so the final result Eq. 21 is obtained upon using

$$\lim_{\rho\to\infty}\rho^2 p_\rho(t) = \int_0^\infty P_4(r,t)2r\,dr \equiv q(t).$$

Supported by Australian Research Council grant AC9330365.

REFERENCES

Abramowitz, M., and I. A. Stegun, editors. 1965. Handbook of Mathematical Functions. Dover, New York.

Akert, K. 1973. Dynamic aspects of synaptic ultrastructure. *Brain Res.* 49:511–518.

Akert, K., H. Moor, and K. Pfenninger. 1971. Synaptic fine structure. *Adv. Cytopharmacol.* 1:273–290.

Augustine, G. J., E. M. Adler, and M. P. Charlton. 1991. The calcium signal for transmitter secretion from presynaptic nerve terminals. *Ann. N.Y. Acad. Sci.* 635:365–381.

Augustine, G. J., and M. P. Charlton. 1986. Calcium-dependence of presynaptic calcium current and post-synaptic response at the giant squid synapse. *J. Physiol.* 381:619–640.

Augustine, G. J., M. P. Charlton, and S. J. Smith. 1985. Calcium entry and transmitter release at voltage-clamped nerve terminals of squid. *J. Physiol.* 367:163–181.

Augustine, G. J., M. P. Charlton, and S. J. Smith. 1987. Calcium action in synaptic transmitter release. *Annu. Rev. Neurosci.* 10:633–693.

Bekkers, J. M., C. B. Richerson, and C. F. Stevens. 1990. Origin of variability in quantal size in cultured hippocampal neurones and hippocampal slices. *Proc. Natl. Acad. Sci. USA.* 87:5359–5362.

Bennett, M. R. 1972. Autonomic Neuromuscular Transmission. Monographs of the Physiological Society: Cambridge University Press, Cambridge, UK.

Bennett, M. R. 1993. The probability of quantal secretion at visualized varicosities of sympathetic nerve terminals. *News Physiol. Sci.* 8:199–201.

Bennett, M. R. 1994. Quantal secretion from single visualized varicosities of sympathetic nerve terminals. *In* Molecular and Cellular Mechanisms of Neurotransmitter Release. L. Stjärne, P. Greengard, S. Grillner, T. Hökfelt and D. Ottoson, editors. Raven Press, New York. 399–423.

Bennett, M. R. 1995. The origin of Gaussian distributions of synaptic potentials. *Prog. Neurobiol.* In press.

Bennett, M. R., C. Fisher, T. Florin, M. P. Quine, and J. Robinson. 1977. The effect of calcium ions and temperature on the binomial parameters that control acetylcholine release by a nerve impulse at amphibian neuromuscular junctions. *J. Physiol.* 271:641–672.

Bennett, M. R., T. Florin, and A. G. Pettigrew. 1976. The effect of calcium ions on the binomial statistical parameters that control acetylcholine release at preganglionic nerve terminals. *J. Physiol.* 257:597–620.

Bennett, M. R., and A. G. Pettigrew. 1975. The formation of synapses in amphibian striated muscle during development. *J. Physiol.* 252: 203–239.

Berridge, M. J. 1992. Cytosolic Ca^{2+} spiking: mechanisms and functional significance. *Neurosci. Facts. Fidia Res. Found.* 3:73–74.

Blackman, J. G., B. L. Ginsborg, and C. Ray. 1963. Spontaneous synaptic activity in sympathetic ganglion cells of the frog. *J. Physiol.* 167: 389–401.

Blackman, J. G., and R. D. Purves. 1969. Intracellular recordings from ganglia of the thoracic sympathetic chain of the guinea-pig. *J. Physiol.* 203:173–198.

Bornstein, J. C. 1981. Effects of stimulation on the multiquantal spontaneous synaptic potentials in guinea-pig hypogastric ganglia. *Neurosci. Lett.* 22:57–61.

Cohen, I. S., W. van der Kloot, and S. B. Barton. 1981. Bursts of miniature endplate potentials can be released from localized regions of the frog nerve terminal. *Brain Res.* 221:382–386.

Couteaux, R. 1961. Principaux critères morphologiques et cytochimiques utilisables aujourd'hui pour définir les divers types de synapses. *Actual. Neurophysiol.* 3:145–173.

de Luca, A., C. G. Li, M. J. Rand, J. J. Reid, P. Thaina, and H. K. Wong-Dusting. 1990. Effects of omega-conotoxin GV IA on autonomic neuroeffector transmission in various tissues. *Brit. J. Pharmacol.* 101: 437–447.

del Castillo, J., and B. Katz. 1954. Quantal components of the end-plate potential. *J. Physiol.* 124:560–573.

Delcour, A. H., D. Lipscombe, and R. W. Tsien. 1993. Multiple modes of N-type calcium channel activity distinguished by differences in gating kinetics. *J. Neurosci.* 13:181–194.

Dennis, M. J., A. J. Harris, and S. W. Kuffler. 1971. Synaptic transmission and its duplication by focally applied ACh in parasympathetic neurones in the heart of the frog. *Proc. R. Soc. Lond. B. Biol. Sci.* 177:509–539.

Dodge, F. A., and R. Rahamimoff. 1967. Co-operative action of calcium ions in transmitter release at the neuromuscular junction. *J. Physiol.* 193:419–432.

Dreyer, F. K., K. Peper, K. Akert, C. Sandri, and H. Moor. 1973. Ultrastructure of the active zone in the frog neuromuscular junction. *Brain Res.* 62:373–380.

Edwards, F. A., A. Konnerth, and B. Sakmann. 1990. Quantal analysis of inhibitory synaptic transmission in the dentate gyrus of rat hippocampal slices: a patch-clamp study. *J. Physiol.* 430:213–247.

Ellinor, P. T., Jc-F. Zhang, A. D. Randall, M. Zhou, T. L. Schwarz, R. W. Tsien, and W. A. Horne. 1993. Functional expression of a rapidly inactivating neuronal calcium channel. *Nature.* 363:455–458.

Erxleben, C., and M. E. Kriebel. 1988. Subunit composition of the spontaneous miniature endplate currents at the mouse neuromuscular junction. *J. Physiol.* 400:659–676.

Fatt, P., and B. Katz. 1952. Spontaneous subthreshold activity at motor nerve endings. *J. Physiol.* 117:109–128.

Feller, W. 1950. An Introduction to Probability Theory and its Applications, Vol. 1, 3rd ed. Wiley, New York.

Fogelson, A. L., and R. S. Zucker. 1985. Presynaptic calcium diffusion from various arrays of single channels: implications for transmitter release and synaptic facilitation. *Biophys. J.* 48:1003–1017.

Fox, A. P., M. C. Nowycky, and R. W. Tsien. 1987. Single-channel recordings of three types of calcium channels in chick sensory neurones. *J. Physiol.* 394:173–200.

Gabella, G. 1992. Fine structure of post-ganglionic nerve fibres and autonomic neuroeffector junctions. *In* Autonomic Neuroeffector Mechanisms. G. Burnstock and C. H. V. Hoyle, editors. Harwood Academic Publishers, Reading, PA. 1–31.

Goda, Y., and C. F. Stevens. 1994. Two components of transmitter release at a central synapse. *Proc. Natl. Acad. Sci. USA.* 91:12942–12946.

Grinnell, A. D., and P. A. Pawson. 1989. Dependence of spontaneous release at frog junctions on synaptic strength, external calcium and terminal length. *J. Physiol.* 418:397–410.

Gulyas, A. I., R. Miles, A. Sik, K. Toth, N. Tanamaki, and T. F. Freund. 1993. Hippocampal pyramidal cells excite inhibitory neurons through a single release site. *Nature.* 366:683–687.

Heidelberger, R., C. Heinemann, E. Neher, and G. Matthews. 1994. Calcium dependence of the rate of exocytosis in a synaptic terminal. *Nature.* 371:513–515.

Heinemann, C., R. H. Chow, E. Neher, and R. S. Zucker. 1994. Kinetics of the secretory response in bovine chromaffin cells following flash photolysis of caged calcium. *Biophys. J.* 67:2546–2557.

Heuser, J. E., and T. S. Reese. 1973. Evidence for recycling of synaptic vesicle membrane during transmitter release at the frog neuromuscular junction. *J. Cell. Biol.* 57:315–344.

Heuser, J. E., T. S. Reese, M. J. Dennis, Y. Jan, L. Jan, and L. Evans. 1979. Synaptic vesicle exocytosis captured by quick freezing and correlated with quantal transmitter release. *J. Cell. Biology.* 81:275–300.

Horne, A. L., and J. A. Kemp. 1991. The effect of ω-conotoxin GVIA on synaptic transmission within the nucleus accumbens and hippocampus of the rat in vitro. *Br. J. Pharmacol.* 103:1733–1739.

Hubbard, J. I., S. F. Jones, and E. M. Landau. 1968. On the mechanism by which calcium and magnesium affect the spontaneous release of transmitter from mammalian motor nerve terminals. *J. Physiol.* 194: 355–380.

Kerr, L. M., and D. Yoshikami. 1984. A venom peptide with a novel presynaptic blocking action. *Nature.* 308:282–284.

Ko, C.-P. 1985. Formation of the active zone at developing neuromuscular junctions in larval and adult bullfrogs. *J. Neurocytol.* 14:487–512.

Korn, H., C. Sur, S. Charpier, P. Legendre, and D. Faber. 1994. The one-vesicle hypotheses and multivesicular release. *In* Molecular and Cellular Mechanisms of Neurotransmitter Release. L. Stjärne, P. Greengard, S. Grillner, T. Hökfelt and D. Ottoson, editors. Raven Press, New York. 301–321.

Kriebel, M. E., and C. E. Gross. 1974. Multimodal distribution of frog miniature endplate potentials in adult, denervated and tadpole leg muscle. *J. Gen. Physiol.* 64:85–103.

Kriebel, M. E., F. Llado, and D. R. Matteson. 1982. Histograms of the unitary evoked potential of the mouse diaphragm show multiple peaks. *J. Physiol.* 322:211–222.

Lavidis, N. A., and M. R. Bennett. 1992. Probabilistic secretion of quanta from vizualized sympathetic varicosities in mouse vas deferens. *J. Physiol.* 454:9–26.

Llinás, R., I. Z. Steinberg, and K. Walton. 1981a. Presynaptic calcium currents in squid giant synapse. *Biophys. J.* 33:289–322.

Llinás, R., I. Z. Steinberg, and K. Walton. 1981b. Relationship between presynaptic calcium current and postsynaptic potential in squid giant synapse. *Biophys. J.* 33:323–352.

Llinás, R., M. Sugimori, D. E. Hillman, and B. Cherksey. 1992. Distribution and functional significance of the P-type voltage dependent Ca^{2+}-channels in the mammalian central nervous system. *Trends Neurosci.* 15:351–355.

Lo, Y., T. Wang, and M. Poo. 1991. Repetitive impulse activity potentiates spontaneous acetylcholine secretion at developing neuromuscular synapses. *J. Physiol. Paris.* 85:71–78.

Luebke, J. I., K. Dunlap, and T. J. Turner. 1993. Multiple calcium channel types control glutaminergic synaptic transmission in the hippocampus. *Neuron.* 11:895–902.

Lux, H. D., and A. M. Brown. 1984. Patch and whole cell calcium currents recorded simultaneously in snail neurons. *J. Gen. Physiol.* 83: 727–750.

MacLeod, G., N. A. Lavidis, and M. R. Bennett. 1994. Calcium dependence of quantal secretion from visualized sympathetic nerve varicosities on the mouse vas deferens. *J. Physiol.* 480:61–70.

Markus, E. J., T. L. Petit, and J. C. Le Boutillier. 1987. Synaptic structural changes during development and aging. *Dev. Brain Res.* 35:239–248.

McLachlan, E. N. 1975. An analysis of the facilitated release of acetylcholine from preganglionic nerve terminals. *J. Physiol.* 245: 447–466.

Melamed, N., P. J. Helm, and R. Rahamimoff. 1993. Confocal microscopy reveals coordinated calcium fluctuations and oscillations in synaptic boutons. *J. Neurosci.* 13:632–649.

Mintz, I. M., M. E. Adams, and B. P. Bean. 1992. P-type calcium channels in rat central and peripheral neurones. *Neuron.* 9:85–95.

Morse, P. M., and H. Feshbach. 1953. Methods of Theoretical Physics. McGraw-Hill, New York.

Parnas, H., G. Hovav, and I. Parnas. 1989. Effect of Ca^{2+} diffusion on the time course of neurotransmitter release. *Biophys. J.* 55:859–874.

Paulsen, P., and P. Heggelund. 1994. The quantal size at retinogeniculate synapses determined from spontaneous and evoked EPSCs in guinea-pig thalamic slices. *J. Physiol.* 480:505–511.

Plummer, M. R., D. E. Logothetis, and P. Hess. 1989. Elementary properties and pharmacological sensitivities of calcium channels in mammalian peripheral neurones. *Neuron.* 2:1453–1463.

Pumplin, D. W., T. S. Reese, and R. Llinas. 1981. Are the presynaptic membrane particles the calcium channels? *Proc. Natl. Acad. Sci. USA.* 78:7210–7213.

Robinson, J. 1976. Estimates of parameters for a model of transmitter release at synapses. *Biometrics.* 32:61–68.

Robitaille, R., E. M. Adler, and M. P. Charlton. 1990. Strategic location of calcium channels at transmitter release sites of frog neuromuscular synapses. *Neuron.* 5:773–779.

Rotschenker, S., and R. Rahamimoff. 1970. Neuromuscular synapse: stochastic properties of spontaneous release of transmitter. *Science.* 170: 648–649.

Silver, R. A., S. F. Traynelis, and S. G. Cull-Candy. 1992. Rapid-time-course miniature and evoked excitatory currents at cerebellar synapses in situ. *Nature.* 355:163–166.

Simon, S. M., and R. R. Llinás. 1985. Compartmentalization of the submembrane calcium activity during calcium influx and its significance in transmitter release. *Biophys. J.* 48:485–498.

Smith, S. J., G. J. Augustine, and M. P. Charlton. 1985. Transmission at voltage-clamped giant synapse of the squid: evidence for cooperativity of presynaptic calcium action. *Proc. Natl. Acad. Sci. USA.* 82: 622–625.

Streichert, L. C., and P. B. Sargent. 1989. Bouton ultrastructure and synaptic growth in a frog autonomic ganglion. *J. Comp. Neurol.* 281: 159–168.

Südhof, T. C., and R. Jahn. 1991. Proteins of synaptic vesicles involved in exocytosis and membrane recycling. *Neuron* 6:665–677.

Triller, A., and H. Korn. 1982. Transmission at a central inhibitory synapse. III. Ultrastructure of physiologically identified and stained terminals. *J. Neurophysiol.* 48:708–736.

Turner, T. J., M. E. Adams, and K. Dunlap. 1993. Multiple Ca^{2+} channel types coexist to regulate synaptosomal neurotransmitter release. *Proc. Nat. Acad. Sci. USA.* 90:9518–9522.

Usowicz, M. M., M. Sugimori, B. Cherksey, and R. Llinas. 1992. P-type calcium channels in the somata and dendrites of adult cerebellar Purkinje cells. *Neuron.* 9:1185–1199.

Van der Kloot, W. 1988. The kinetics of quantal release during end-plate currents at the frog neuromuscular junction. *J. Physiol.* 402:605–626.

Vautrin, J., and M. E. Kriebel. 1991. Characteristics of slow-minature end-plate currents show a subunit composition. *Neuroscience.* 41: 71–88.

Wheeler, D. B., W. A. Sather, A. Randall, and R. W. Tsien. 1994. Distinctive properties of a neuronal calcium channel and its contribution to excitatory synaptic transmission in the central nervous system. pp. 155–172. *In* Cellular and Molecular Mechanisms of Neurotransmitter Release. L. Stjärne, P. Greengard, S. Grillner, T. Hökfelt and D. Ottoson, editors. Raven Press, New York.

Yamada, W. M., and R. S. Zucker. 1992. Time course of transmitter release calculated from simulations of a calcium diffusion model. *Biophys. J.* 61:671–682.

Zucker, R. S., and A. L. Fogelson. 1986. Relationship between transmitter release and presynaptic calcium influx when calcium enters through discrete channels. *Proc. Natl. Acad. Sci. USA.* 83:3032–3036.